



## Current-Injected Mode Control for Coupled-Inductor (Ci) Based Boost Converter

Ansa Nawaz<sup>1</sup>, Taosif Iqbal<sup>1</sup>, Nabila Nawaz<sup>2</sup>

<sup>1</sup>Department of Electrical Engineering, College of Electrical & Mechanical Engineering (E&ME), Rawalpindi Pakistan

<sup>2</sup>Department of Electrical Engineering, Ghulam Ishaq Khan Institute of Engineering Sciences and Technology Pakistan

\*Correspondence: [ansanawaz96@gmail.com](mailto:ansanawaz96@gmail.com); [taosifiqbal@ceme.nust.edu.pk](mailto:taosifiqbal@ceme.nust.edu.pk); [nabilakcp@gmail.com](mailto:nabilakcp@gmail.com)

**Citation** | Nawaz. A, Iqbal. T, Nawaz. N, “Current-Injected Mode Control for Coupled-Inductor (Ci) Based Boost Converter”, IJIST, Special Issue pp 01-17, March 2025

**Received** | Feb 08, 2025 **Revised** | Feb 20, 2025 **Accepted** | March 25, 2025 **Published** | March 01, 2025.

With the increasing demand for electrical energy, there is a need to replace conventional energy resources with renewable energy resources. To properly implement renewable resources at a larger scale, DC/DC converters play a major role. Owing to the variable and unreliable nature of renewable energy resources like PV systems there is a requirement for converters that can regulate the voltage at the output side. High-gain DC/DC converters are preferred for the integration of the solar system in smart grids or microgrids. In this context, a high-gain boost converter utilizing a coupled inductor is a preferable choice. High gain is achieved by the proper selection of the turn's ratio of coupled inductors in such converters. Whereas to obtain voltage regulation there is a need to employ an effective control scheme. In this paper current-injected control topology has been utilized for coupled inductor-based boost converter. The proposed converter with an appropriate control scheme aims to achieve high voltage gain, reduced switching losses, minimization of current ripple, and less conduction losses while increasing the efficiency of the overall system. A small signal model based on the state space averaging technique is used to derive control to output transfer function for the proposed converter. A hardware prototype has been implemented for the validation of theoretical work. The overall efficiency of the converter is calculated to be around 96% at specific load conditions.

**Keywords:** Coupled Inductor, Non-Isolated Converter, Small Signal Modeling, Current Mode Control, High Gain Converter, Dc-Dc Boost Converter



## Introduction:

Renewable energy resources have gained immense attention due to the depletion of conventional energy resources like fossil fuels. The increasing environmental issues have also made it necessary to look for resources that can provide clean energy. The growing trend towards industrialization, urbanization, and an increase in population requires sustainable and eco-friendly energy resources to meet the energy demand [1]. Renewable energy resources like wind, solar, or fuel cells are a source of sustainable energy that has a positive impact on the environment. Renewable energy resources can develop a distributed energy system/hybrid system that can provide decentralized energy [2]. The integration of renewable energy resources requires DC-DC converters that can efficiently boost the low terminal voltage.

Due to the fluctuating and low output voltage of RES, the role of DC-DC power electronic boost converters is significant [3]. The proper selection of such converters depends on various factors like the elements (size), efficiency, and voltage gain [4], [5]. Ripple in the input current, voltage and current stress on the switch also play an imperative role. To implement MPPT for PV the high ripple in the input current is problematic and undesirable [6]. In comparison to transformer-based isolated DC-DC converters, non-isolated DC-DC converters are preferable. Some of the issues associated with isolated converters include voltage stress on the switch, core saturation, and voltage spikes due to the leakage inductor of the transformer [7].

Conventional boost converters aren't compatible with applications that require high voltage. Although the voltage gain of a conventional boost converter can be increased by setting a high value of duty ratio. But then again, the higher value of the duty cycle causes conduction losses, voltage stress on the switch, reverse recovery issue of the diode, and large ripple in inductor current. It is uneconomical and impractical to use a conventional boost converter with a high value of duty ratio. The requirement of high rating switches requiring large ON-state resistance, the impact of ESR (equivalent series resistor) of the inductor, and electromagnetic interface limit the use of CBC [8],[9].

Various converters have been suggested that involve transformers to achieve high voltage gain [10],[11]. Isolated converters based on transformers can achieve high voltage with a low duty ratio, but these topologies are costly and require multistage power conversion. Voltage lift techniques have also been implemented [12]. Switched inductor-based converters can achieve high gain [13] but require a large count of components especially magnetic devices/inductors and a couple of diodes. Similarly, active network converters based on switched capacitors can also be used in high-voltage applications but require two switches along with the circuitry of the gate drive which increases overall cost [14]. Coupled inductor-based step-up converters are preferred to achieve the goal of high gain and low voltage stress [15] but the main problem is the high current ripple and no control for voltage regulation. Some topologies utilize coupled inductor to overcome the issue of voltage stress and current ripple but require large number of components [16],[17].

In this paper, a coupled inductor boost converter based on current mode control has been proposed to achieve high gain, efficiency, and voltage regulation. By properly adjusting the turns ratio of the coupled inductor high gain can be achieved but it causes a voltage spike and high ripple current. To overcome this problem current mode control CMC or current-injected control is implemented which is comprised of an outer loop (voltage control) and an inner loop (current control). The proposed converter aims to achieve the goals of high gain, high efficiency no reverse recovery issues, and less power/conduction losses. Boost converter has a problem of non-minimum phase that is due to the presence of zero in the right half s-plane. The voltage regulation is also an important factor for PV applications due to variations and unreliable terminal voltage. To deal with all such problems dual loop control is utilized. Current mode

control is usually preferred over-voltage mode control due to the slow response of VMC w.r.t load variations. The proposed converter aims to achieve the following goals:

1. High gain & high overall efficiency.
2. Minimum count of magnetizing and switching components.
3. Implantation of a simple and robust control structure to reduce current ripples.
4. Voltage regulation, stability, and reliability.

The main objective of this research is to develop a highly efficient, high-gain CI (coupled-inductor) based boost converter utilizing a current-injected control for voltage regulation and stability. By optimizing the turns ratio, the design minimizes switching losses and reduces duty cycle constraints, ensuring improved voltage conversion efficiency. A dual-loop feedback control mechanism is implemented, comprising an inner current loop for fast transient response and an outer voltage loop for precise regulation. This approach effectively suppresses voltage oscillations, electromagnetic interference (EMI), transient overshoots, and peak inductor currents, maintaining a steady output voltage despite input fluctuations. The proposed system is particularly beneficial for renewable energy sources like photovoltaic (PV) systems & fuel cells, where stable power conversion is essential.

This work presents a current-injected mode control for a coupled inductor boost converter, offering enhanced voltage gain, dynamic response, and noise immunity. Unlike conventional boost converters, this design reduces switching stress by achieving high gain at lower duty cycles. The dual-loop control strategy effectively addresses right-half-plane (RHP) zero instability, ensuring system stability. Additionally, a compensation-ramp technique is integrated to suppress subharmonic oscillations, enhancing phase margin and gain characteristics without additional passive components. The proposed converter is validated through MATLAB/Simulink simulations and hardware implementation, demonstrating superior efficiency, transient response, and total harmonic distortion (THD) reduction, making it ideal for renewable energy and electric vehicle (EV) charging applications.

The paper has been divided into different sections for the convenience of the reader. Section 2 includes the basic introduction of the coupled inductor and the working principle of the proposed converter. In section 3 small signal model based on the state space averaging technique is used to derive control of the output transfer function. Section 4 covers the implementation of a current-injected control scheme to achieve voltage regulation and stability. It also gives a brief comparison of voltage mode control with current-injected mode control. Section 5 defines the effectiveness of the proposed converter in comparison to relevant converters that have been proposed in recent years. Section 6 involves the simulation results obtained via Matlab/Simulink as well as the hardware results that validate the theoretical work and performance of the proposed converter. Section 7 is the last section of this paper which includes future recommendations and conclusions.

## **Methodology:**

### **Basic Understanding & Working of the Proposed Converter:**

The basic circuit diagram of the proposed converter is shown in Figure 1. The replacement of the coupled inductor with a boost converter helps to achieve high gain. There are 2 modes of operations based on the state (ON/OFF) of the switch (MOSFET) during the switching period. The converter is merely comprised of the coupled inductor at the input side, high rating MOSFET, diode, capacitor, and resistive load at the output. The subsections define detailed working requirements and modes of operation. The basic understanding of coupled inductors is also briefly defined. The converter has been operated in the continuous conduction mode for simplicity.

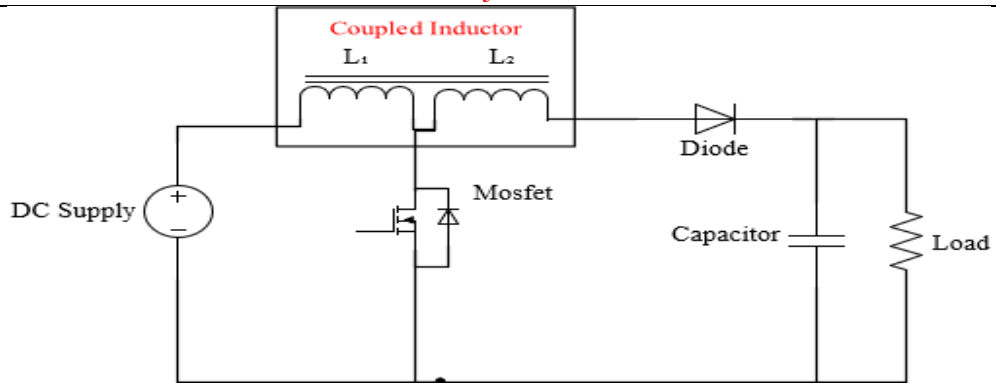


**Figure 1.** Coupled inductor-based step-up high gain boost converter [18]

Coupled inductors are used to achieve high gain without utilizing the high value of duty cycle i.e., duty cycle  $d > 70\%$ . On the other hand, wire resistance associated with the inductor introduces a limit on the selection of the duty cycle. In the case of a conventional boost converter increase in duty cycle to get high gain affects the overall efficiency. One option can be to use a wire of thick diameter, but it results in increased conduction losses with more current stress. The reverse recovery problem of the diode becomes predominant. At the same time reverse voltage appearing during the off state becomes larger in value and introduces conduction losses. Therefore, to overcome such problems coupled inductors are utilized. They simply have double winding at the same core instead of single winding. It helps to not only achieve high gain but also reduces conduction/switching losses with less voltage stress [18].

**Operation modes (ON & OFF Position of MOSFET/Switch) for the Proposed Converter:**

The two modes of operation have been shown with equivalent circuit diagrams for the ON and OFF states of the switch (MOSFET). In 1<sup>st</sup> mode of operation, as shown in Figure 2 (a), the switch (MOSFET) is in the ON state, and thus the 1<sup>st</sup> coil of the inductor stores energy through the source. In this state the diode gets open (reverse biased). While in the 2<sup>nd</sup> state of operation, as shown in Figure 2 (b), the diode gets forward-biased, and the switch (MOSFET) is in the OFF state. During this duration, the energy is delivered to the capacitor, and the load is connected in parallel via a diode which is conducting. In 2<sup>nd</sup> mode of operation, the 2 coils of the coupled inductor get in series thus same current flows through them.

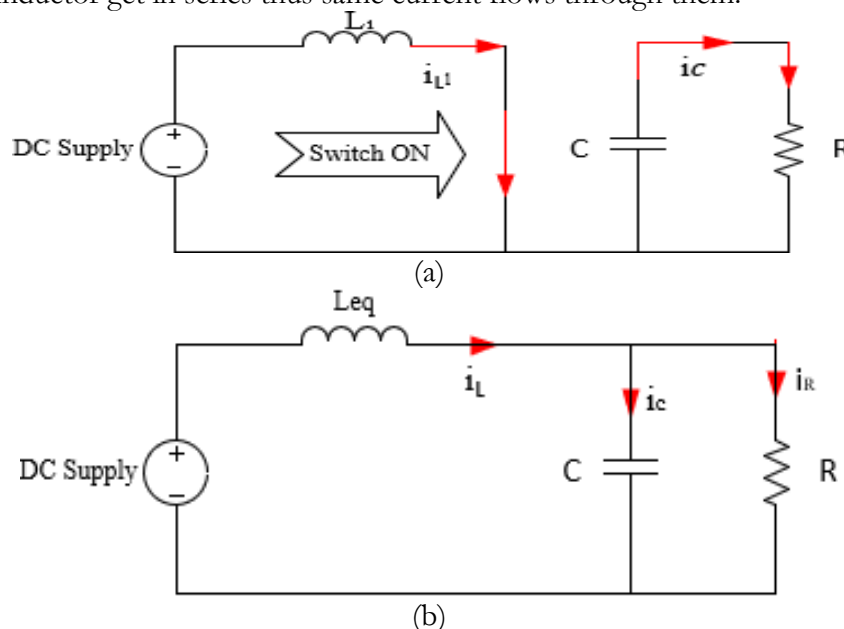


**Figure 2** (a). Equivalent circuit for 1<sup>st</sup> mode (b) Equivalent circuit for 2<sup>nd</sup> mode

**Mathematical Modeling Based on 2 Modes of Operation:**

In 1<sup>st</sup> mode, energy gets stored through an input (DC) supply in L<sub>1</sub> when the switch (MOSFET) is in the ON state. In this state, the diode gets in a reversed biased state. The voltage applied across 1 coil eventually causes the voltage across the other coil that is linked magnetically to the 1<sup>st</sup> coil. Let the voltage across 1<sup>st</sup> coil be represented as v<sub>11</sub> and can be given as:

$$v_{11} = L_1 \cdot \frac{di_{11}}{dt} \quad (1)$$

The term L<sub>1</sub> indicates the inductance related to 1<sup>st</sup> coil and is termed the self-inductance of that coil. The change in current causes a flux in the common core around which 2 coils are being wound. The flux can be represented as:

$$\Phi = i_{11} * c * N_{11} \quad (2)$$

Here, c is dependent on the core's geometry and magnetic properties whereas N<sub>11</sub> is no. of turns of 1<sup>st</sup> coil. It is to be noted that flux is contained and linked with the common core. The voltage and flux relation for 1<sup>st</sup> coil is given as [19]:

$$v_{11} = N_{11} \cdot \frac{d\Phi_{11}}{dt} \quad (3)$$

Similarly, for the 2<sup>nd</sup> coil the induced voltage or emf while considering that flux is the same in both the 1<sup>st</sup> as well as 2<sup>nd</sup> coil, the expression for induced voltage in the 2<sup>nd</sup> coil is:

$$v_{12} = M_1 \cdot \frac{di_{11}}{dt} \quad (4)$$

Here the term M<sub>1</sub> is the mutual inductance among the 2 coils wound at the same core to form couple-inductor with the units same as inductance i.e., Henry- 'H'. The term c depends upon the core's properties. The voltage induced in 2<sup>nd</sup> coil can also be given as:

$$v_{12} = n \cdot v_{in} \quad (5)$$

In 2<sup>nd</sup> state of operation, the switch gets open (OFF state) and the diode gets forward biased. The voltage across 1<sup>st</sup> coil is:

$$v_{11} = \frac{N_{11} \cdot (v_o - v_{in})}{N_{11} + N_{12}} \quad (6)$$

Whereas the equivalent inductance is represented by L<sub>equ</sub> is given as:

$$L_{equ} = L_1 + L_2 + (2 * M) \quad (7)$$

$$L_{equ} = L_1 \cdot (1 + n)^2 \quad (8)$$

The relation between inductors L<sub>1</sub>, L<sub>2</sub>, and turns ratio can be expressed as

$$n^2 = (N_{12}/N_{11})^2 = L_2/L_1 \quad (9)$$

The concept of coupled inductors is quite simple as it utilizes a single core with 2 inductors wound on it. The turns ratio is selected according to the desired application and the connection of windings can either be in parallel or series as per requirement. The turn ratio can be higher depending on the design specifications. Mutual inductance also plays an important role in the overall performance of the coupled inductor. The value of k (coupling coefficient of the coupled inductor) is chosen between 0.95 & 0.99. Typically, its value is chosen as k=0.95. Where the coupling coefficient and mutual inductance are related as:

$$M = (\sqrt{L_1 \cdot L_2}) \cdot k \quad (10)$$

**State Space Modeling:**

Using the equivalent models of proposed converters based on ON as well as OFF states. State space-based modeling with matrix algebra makes it easy to understand the overall system design. It is usually based upon 1<sup>st</sup> order differential equations that model inductors and capacitor's current and voltage respectively. The calculations are based mainly on the time domain and the overall system is represented in the format of matrix.

The basic equation form for such a system is mainly given as:

$$\dot{x} = (A \cdot x) + (B \cdot u) \quad (11)$$

$$Y = C \cdot x \quad (12)$$

1) When the switch is closed, as shown in Figure 3, then it has the following form.

$$\dot{x} = A_{01}x + B_{01}u \quad (13)$$

2) When the switch is open then:

$$\dot{x} = A_{02}x + B_{02}u \quad (14)$$

As per average modeling is concerned then by combining 2 modes as mentioned above, we get the following form:

$$\dot{x} = \overline{A_{av}}x + \overline{B_{av}}u \quad (15)$$

Whereas

$$\overline{A_{av}} = A_{01} \cdot d + A_{02}(1 - d) \quad (16)$$

Similarly

$$\overline{B_{av}} = B_{01} \cdot d + B_{02}(1 - d) \quad (17)$$

Here A represents dynamics for the state of the system and B for the controllable input.

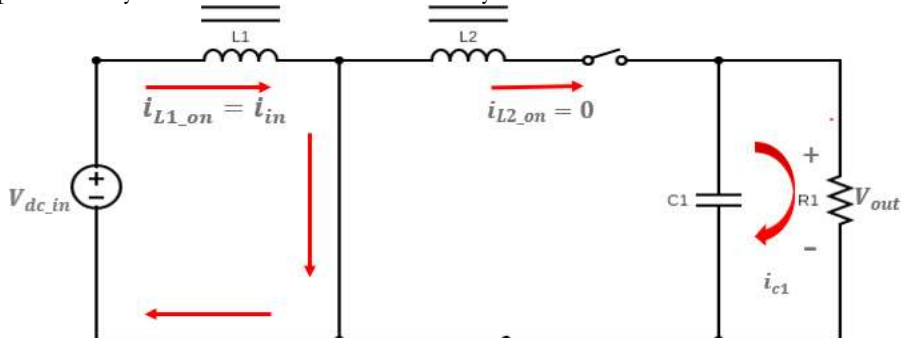


Figure 3. State 1 when the switch is ON

$$x_{1\_on} = i_{L1\_on} \quad (18)$$

$$x_{2\_on} = V_{C\_on} \quad (19)$$

$$\begin{bmatrix} \dot{x}_1 \\ \dot{x}_2 \end{bmatrix} = \begin{bmatrix} 0 & 0 \\ 0 & -\frac{1}{C_1 R_1} \end{bmatrix} \cdot \begin{bmatrix} i_{L1\_on} \\ V_{C\_on} \end{bmatrix} + \begin{bmatrix} \frac{1}{L_1} \\ 0 \end{bmatrix} \cdot V_{dc\_in} \quad (20)$$

$$A_{01} = \begin{bmatrix} 0 & 0 \\ 0 & -\frac{1}{C_1 R_1} \end{bmatrix} \text{ and } B_{01} = \begin{bmatrix} \frac{1}{L_1} \\ 0 \end{bmatrix} \quad (21)$$

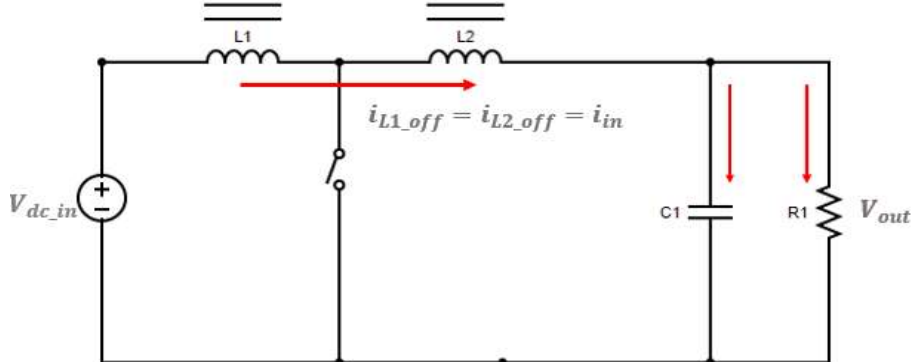


Figure 4. State 2 when the switch is OFF

The state when the switch (MOSFET) is in off state, as shown in Figure 4, then both coils are in series with each other.

$$\frac{dV_{C\_off}}{dt} = \frac{1}{C_1} (i_{L1\_off} - \frac{1}{R_1} (V_{C\_off})) \quad (22)$$

Thus, in mode 2 we have:

$$\frac{di_{L1\_off}}{dt} = \frac{1}{L_{equ}} (V_{dc\_in} - V_{C\_off}) \quad (23)$$

Here notice that  $L_{equ}$  Shows the series combination of both inductors.

The matrix form of the above differential's equations can be:

$$\begin{bmatrix} \dot{x}_1 \\ \dot{x}_2 \end{bmatrix} = \begin{bmatrix} 0 & -\frac{1}{L_{equ}} \\ \frac{1}{C_1} & -\frac{1}{C_1 R_1} \end{bmatrix} \cdot \begin{bmatrix} i_{L1\_off} \\ V_{C\_off} \end{bmatrix} + \begin{bmatrix} \frac{1}{L_{equ}} \\ 0 \end{bmatrix} \cdot V_{dcin} \quad (24)$$

$$A_{02} = \begin{bmatrix} 0 & -\frac{1}{L_{equ}} \\ \frac{1}{C_1} & -\frac{1}{C_1 R_1} \end{bmatrix} \text{ and } B_{02} = \begin{bmatrix} \frac{1}{L_{equ}} \\ 0 \end{bmatrix} \quad (25)$$

Now final step is to combine the 2 states through the averaging method:

$$\dot{x} = \begin{bmatrix} 0 & -\frac{(1-d)}{L_{equ}} \\ \frac{1-d}{C_1} & -\frac{1}{C_1 R_1} \end{bmatrix} \cdot x + \begin{bmatrix} \frac{1}{L_1} (d) + \frac{1}{L_{equ}} (1-d) \\ 0 \end{bmatrix} \cdot V_{dcin} \quad (26)$$

For derivation of the transfer function i.e. control to output requires 2 main parameters that are output or capacitor voltage and inductor's current. Here the input side voltage is taken as disturbance whereas control d (duty cycle) is chosen. Therefore, the state-space model after some modifications is presented generically as:

$$\dot{x}' = \begin{bmatrix} i_{Le} \\ V_{Co} \end{bmatrix} \quad (27)$$

$$\tilde{u}' = \begin{bmatrix} V_{dcin}' \\ d' \end{bmatrix} \quad (28)$$

$$A' = \begin{bmatrix} 0 & -\frac{(1-d)}{L_{equ}(1+n)} \\ \frac{1-d}{C_1(1+n)} & -\frac{1}{C_1 R_1} \end{bmatrix} \quad B' = \begin{bmatrix} \frac{1+(n.d)}{L_{equ}(1+n)} & \frac{V'_{C+n.V_{dcin}'}}{(1+n)} \\ 0 & -\frac{i_{L'}}{C_1(1+n)} \end{bmatrix} \quad (29)$$

The control-to-output transfer function is derived as [18]:

$$G_{V_{C-d}} = \frac{V_{C'}}{d'} = \frac{i'_{L,s} \frac{(1-d')(V'_{C+n.V_{dcin}'})}{(1+n)} + \frac{(n+1)^2}{s^2 + s + \frac{(1-d')}{(1+n)^2 R_1}}}{(1+n)} \quad (30)$$

The subharmonic oscillations play a major role in CMC implementation. A compensation ramp can eliminate this effect of subharmonic oscillations [20]. It is predominant especially when  $d > 0.5$  or 50% which means there is a major instability problem while dealing with current-injected control.

design equations for the compensation ramp slope are given below, ensuring stable operation. In the current injected mode-based coupled inductor boost converter configuration, the ramp compensation is essential to prevent sub-harmonic oscillations that arise when the duty cycle D is set above 50 %. A compensation ramp (Se) is added to the inductor current signal to dampen oscillations and stabilize the current loop. While the slop is introduced into the control signal to counteract duty cycle-dependent oscillations.

$$V_{out} = (1+n) V_{dcin} / (1-d) \quad (31)$$

The required compensation ramp slope Se is:

$$S_e > (S_{off} - S_{on}) / 32 \quad (32)$$

Where:

$S_{on}$  = Slope of the on-time inductor current

$S_{off}$  = Slope of the off-time inductor current

The Slopes for the on-time inductor current is given as:

$$S_{on} = V_{dcin} / L_{equ} \quad (33)$$

The Slopes for the off-time inductor current are given as:

$$S_{off} = [(1+n) V_{dcin} - V_{dcin}] / L_{equ} \quad (34)$$

where  $L_{equ}$  is the equivalent inductance considering coupling effects

$$Se > \frac{(1+n)V_{dcin} - V_{dcin} - \frac{V_{dcin}}{Lequ}}{2} \quad (35)$$

After rearranging the final equation is:

$$Se > \frac{n-1}{2} \cdot \frac{V_{dcin}}{Lequ} \quad (36)$$

The op-amp used for designing frequency-based compensation involves feedback to achieve stability. Type 2 and type 3 compensators are usually preferred for boost converters to implement voltage or current-injected control. Type 2 compensator has an RC network for getting better phase response and flatten gain. Type 3 compensator helps to improve the phase response even further with the addition of 2 poles, 2 zeros, and a pole at zero location [21]. However, the relevant transfer function derived using the simplified block diagram of current-injected control is given as [22]:

$$T.F_{(VC)} = \frac{G_v \cdot K_m}{K_m \cdot [(G_v \cdot K_{vd}) + G_i]} \quad (37)$$

**Results and Discussion:**

**Implementation of the Proposed Converter with Voltage Mode Control:**

Voltage Mode Control (VMC) is a feedback control technique used in power converters to regulate output voltage by comparing the feedback voltage with a reference value as shown in Figure 5. The error signal generated is used to control the duty cycle of a MOSFET via PWM modulation. While VMC is useful in applications with input or load voltage variations, light loads, or when avoiding the complexities of dual-loop control, it faces challenges due to the right-half-plane zero, which complicates loop compensation, especially in boost converters. As a result, VMC is often less effective than Current Mode Control (CMC), which provides more precise control by using the inductor current as a state variable and is preferred in applications requiring fast dynamic response, current sharing, or noise immunity. CMC also offers better stability and efficiency in high-power and multi-phase converters, making it the favored choice in many designs. The voltage mode-based control was implemented on Matlab/Simulink and the output voltage as well as current waveforms are shown in Figure 6.

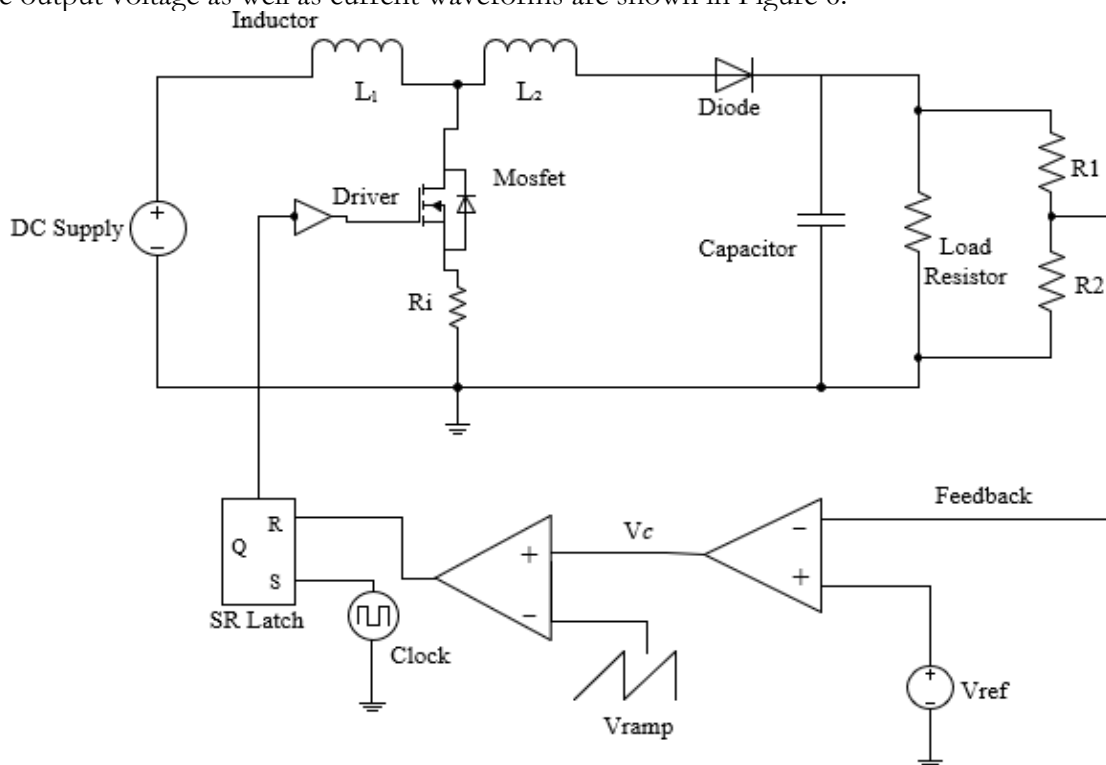


**Figure 5.** Circuit diagram for proposed converter, utilizing VMC

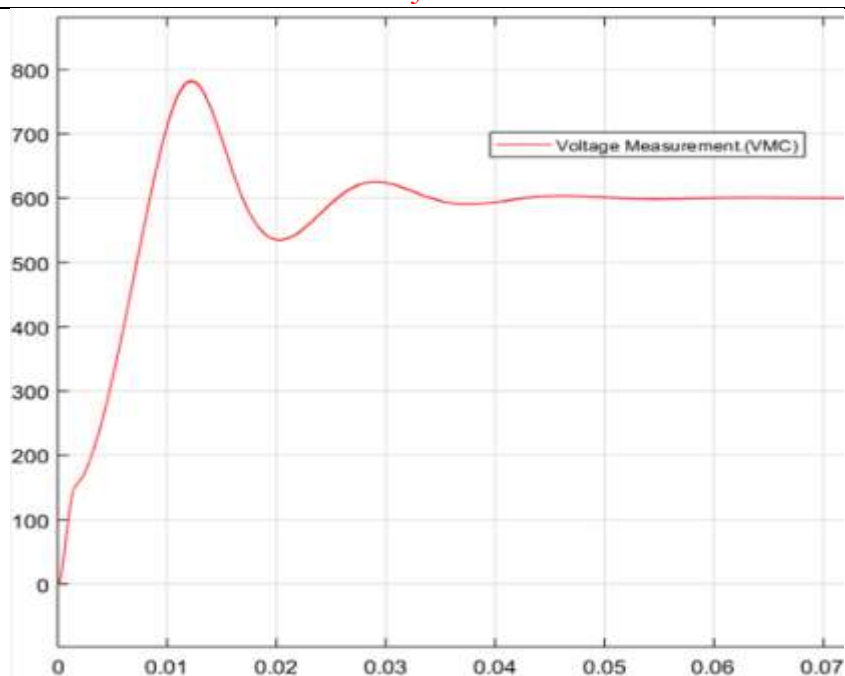


Figure 6. (a) Voltage at the output side

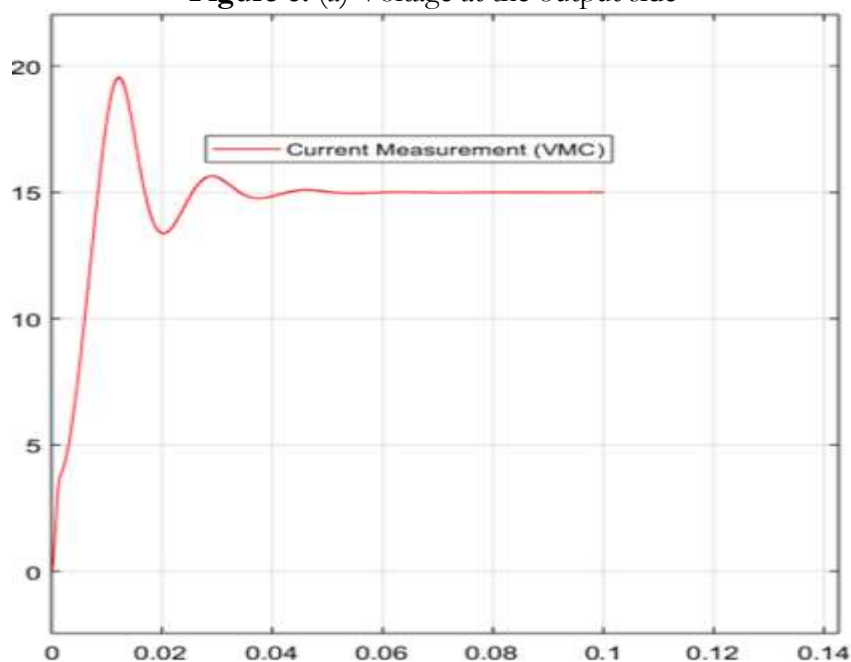
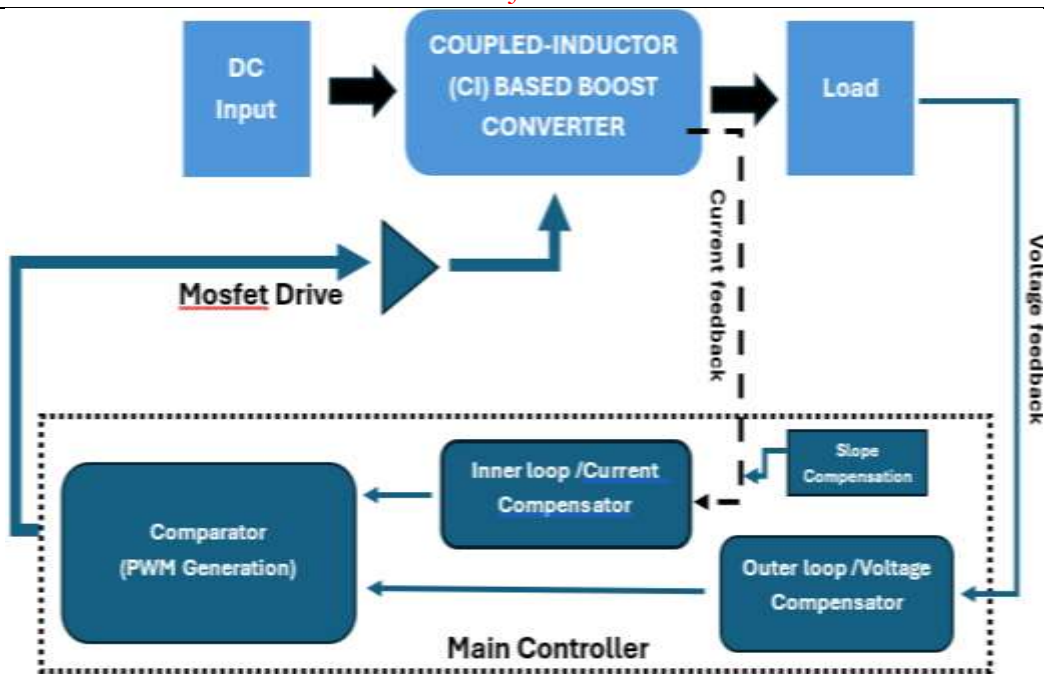


Figure 6. (b) output current  $I_{out}$  for voltage mode-based converter control (VMC) based proposed converter

### Implementation of the proposed converter with the current injected mode control

Current-mode control (CMC) is often preferable over Voltage-Mode Control (VMC) due to its faster dynamic response, particularly under load variations. CMC incorporates two feedback loops as shown in the block diagram for the proposed converter (Figure 7), improving stability and mitigating the impact of right-half s-plane zeros. This enhances transient response and allows for reduced total harmonic distortion (THD) and better input disturbance rejection.



**Figure 7.** Block diagram for current-injected control with current (inner) and voltage (outer) loops

For current-injected mode control the inductor current or switch current is taken as feedback, and it is compared to control current, as shown in the circuit diagram in Figure 8. The current mode-based control design is helpful in not only achieving regulated output voltage but also improving stability as well as transients.

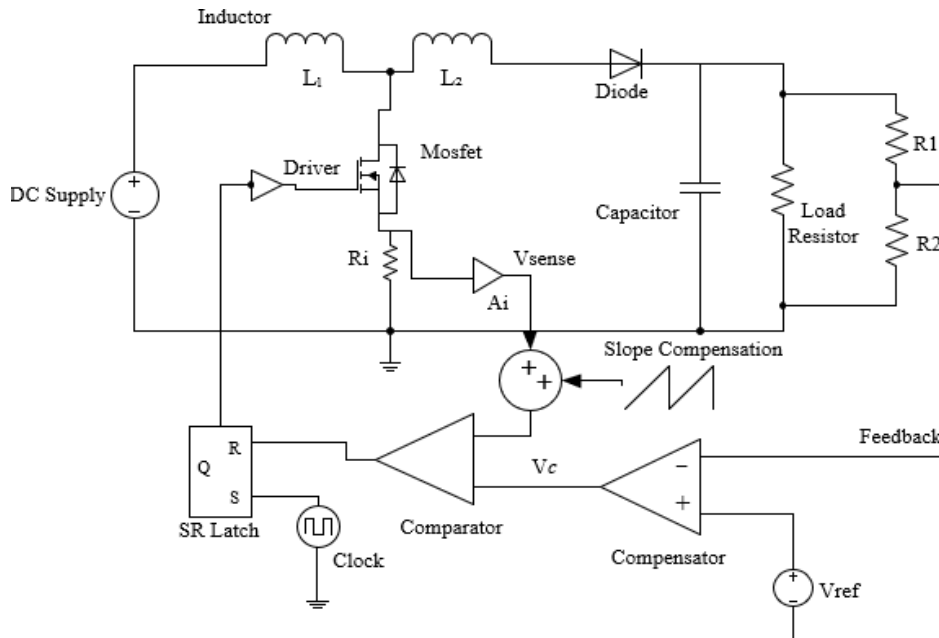


**Figure 8.** Circuit diagram for current-injected control with slope compensation

Type 3 compensation is rather easy, as shown in Figure 9, simplifies rules and achieves stability effectively. The role of ramp involvement is merely to minimize the involvement of subharmonic oscillations. Current injected control methodology is also termed as a current programmed mode which contains a total of 2 loops. Sometimes it's also termed as multiple loop control as it has 2 loops, one being the current loop which is an inner loop and the other is the voltage loop which is an outer loop in the overall control mechanism.

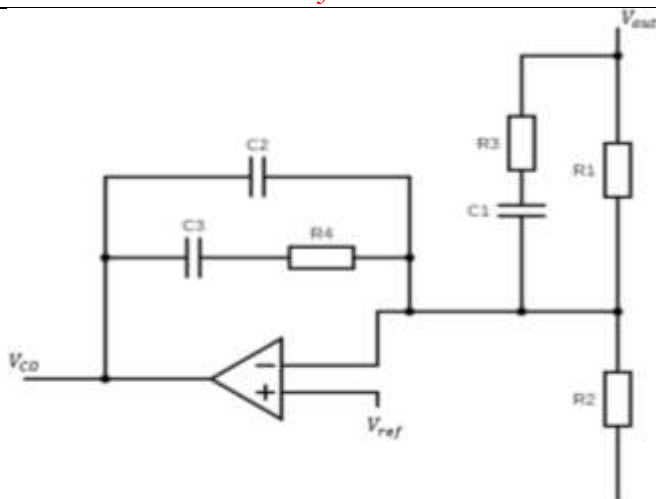


**Figure 9.** Type 3 compensator via op- amp [21]

To relate the control current with the respective output voltage a simplified transfer function is derived using a small signal model. With the addition of compensation/artificial ramp, the difference between the control current and inductor sensed current becomes prominent. In the block diagram, given in Figure 10, the km block represents the role of compensation ramp.

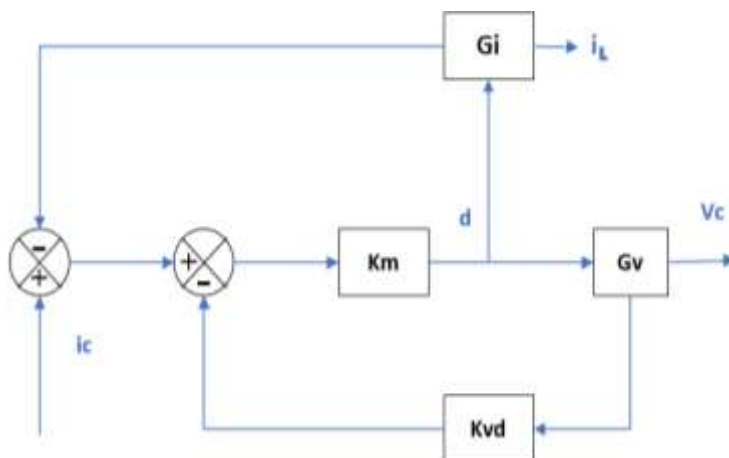


**Figure 10.** Current injected control-based simplified block diagram for the proposed converter

By using a Type-3 compensator, often implemented with an op-amp, CMC can achieve phase boosts greater than  $90^\circ$ , improving stability and performance. Furthermore, CMC limits overcurrent conditions, preventing system failures and offering robust control. In systems with duty cycles greater than 50%, subharmonic oscillations are mitigated by adding a compensation ramp. This makes CMC particularly beneficial for better efficiency, high gain converters that can be utilized for renewable energy system integration, and electric vehicles, where rapid and stable voltage regulation is critical. The overall system for current-injected control with slope compensation was implemented in Matlab/Simulink and its output voltage as well as current waveforms are given in Figure 11.

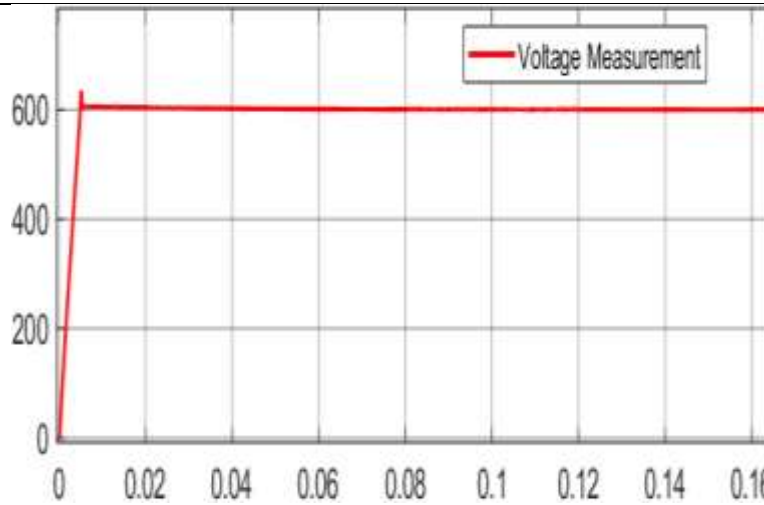


Figure 11(a). Output Voltage waveform of the proposed converter with CMC

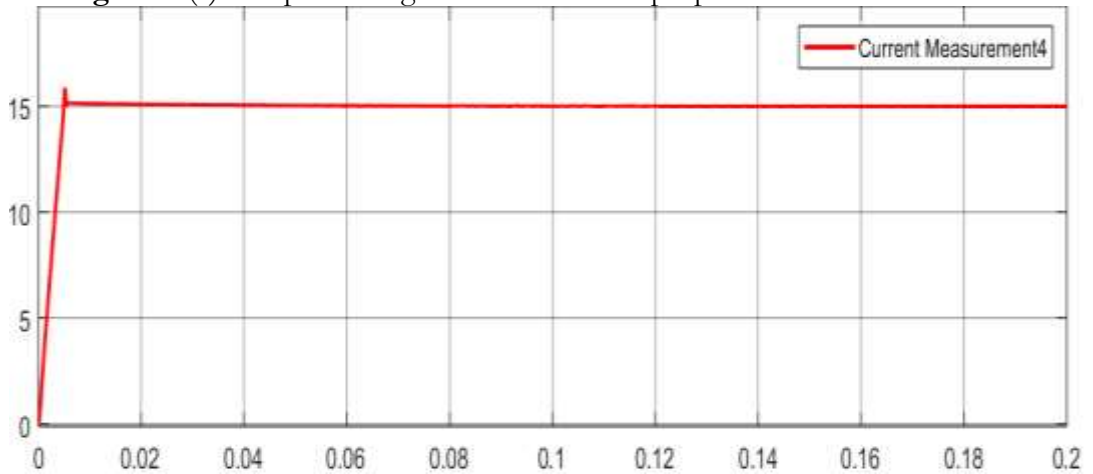


Figure 11 (b). Output Current waveform of the proposed converter with CMC

**Effectiveness of Proposed Converter W.R.T Relevant Converters:**

The major emphasis was to develop a converter that could achieve high gain and efficiency. The comparison has been built to show the effectiveness of the converter as shown in table 01. The comparison has been done based on component count (like for switch, diode, and capacitor), and voltage stress of capacitor and switch. Finally, the converter's voltage gain vs duty ratio curves have been plotted as shown in Figure 12.

**Table 1.** Comparison table of proposed converter with other relevant topologies

Topology	Proposed Converter	Ref [23]	Ref [17]	Ref [15]	
No of switches	1	1	2	1	2
No of capacitors	1	3	2	4	5
No of diodes	1	4	2	4	8
Switch side voltage stress.	$\frac{[1 + n.d]V_i}{(1 - d)}$	$\frac{V_i}{(1 - d)}$	$\frac{[1 + (2n)]V_i}{(1 - d)}$	$\frac{V_i}{(1 - 2.d)}$	$\frac{V_i}{(1 - d)}$
Output capacitor side stress	less	high	high	high	high

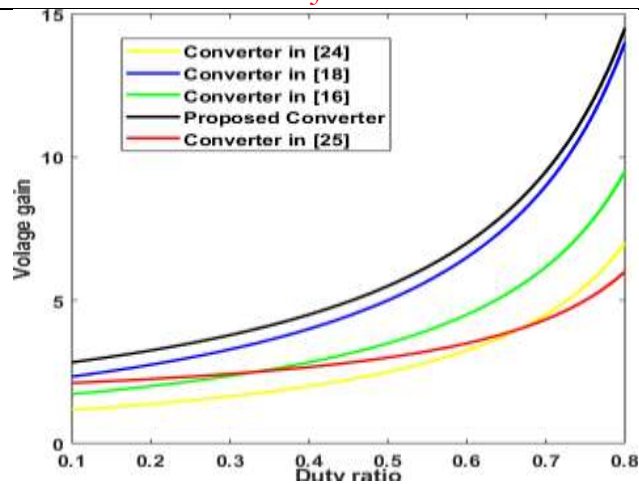


Figure 12. Voltage gain to duty ratio comparison curves

### Discussion:

To testify to the performance of the proposed converter a hardware prototype has been built. The efficiency curve is drawn for various loads varying from 10W to 100W when connected at the load side. For a load of 100W, the overall efficiency is calculated to be around 95- 96% for a voltage of 8-10V at the input side and 97-101V at the output side. The hardware prototype implementation is shown in Figure 13. The selection of components and their values are set as per mathematical calculations as given in Table 02. The high conversion efficiency for the proposed converter has been observed to have a peak value of around 96%. The efficiency vs output power curve is also given in Figure 14.

The output voltage and current waveforms of the proposed Coupled Inductor Boost Converter demonstrated significant improvements over the existing topologies referenced in the literature. Unlike conventional boost converters, where high-duty cycles lead to excessive voltage ripples and instability [8][9], the proposed topology achieves higher voltage gain at moderate-duty cycles, as seen in the voltage waveform, where the output voltage remains stable with minimal overshoot and steady-state error. In contrast to switched capacitors and interleaved boost converters, which experience high inrush currents and increased switching losses [14], [15], the proposed converter maintains a well-regulated and smooth current waveform, reducing stress on power components. Additionally, compared to transformer-based isolated converters, which often suffer from leakage inductance-induced oscillations [10], [11], the proposed design ensures a more controlled voltage response with faster settling time. Implementing current mode control further enhances overall stability by mitigating right-half-plane (RHP) zero effects, ensuring faster transient response and lower current ripples compared to voltage mode control (VMC), as compared in section 4 of the paper where voltage mode control is first separately implemented and then current-injected mode control is implemented, involving both outer (voltage loop) and inner (current loop). Efficiency curves also validate the superiority of this design, showing higher efficiency (>95%) across different load conditions, whereas conventional topologies often exhibit a drop in efficiency due to increased conduction losses. These results confirm that the proposed converter is better suited for renewable energy applications and high-power DC systems, providing stable operation, lower ripple, and improved dynamic response compared to the existing literature.

Various control strategies exist for boost converters, each with unique advantages and limitations in terms of dynamic response, noise rejection, and implementation complexity. While the current study employs current-injected mode control (CMC) to enhance system stability and efficiency, alternative control techniques such as Voltage Mode Control (VMC), Sliding Mode Control (SMC), Predictive Control (MPC), and Fuzzy Logic Control (FLC) have been widely

explored in the existing literature. A comparative analysis of these methods provides valuable insights into their suitability for different power electronics applications.

Voltage Mode Control (VMC) is one of the simplest and most commonly used techniques for regulating the output voltage of a boost converter. It operates using a single feedback loop where the output voltage is compared to a reference, and the error is processed through a compensator, typically generating a pulse-width modulation (PWM) signal. While VMC is easy to implement and cost-effective, it suffers from slow dynamic response and poor noise rejection, making it less effective for applications requiring fast transient regulation. Furthermore, the presence of a right-half-plane (RHP) zero in boost converters complicates loop compensation and limits performance. In comparison, CMC provides faster dynamic response and better noise immunity, as it directly controls the inductor current rather than relying solely on output voltage feedback.

Sliding Mode Control (SMC) is a nonlinear control strategy that dynamically adjusts the duty cycle based on system states, ensuring robust performance even under uncertain conditions. This approach excels in fast transient response and noise rejection, making it ideal for high-performance applications in harsh environments. However, the primary drawback of SMC is the chattering effect, where high-frequency switching introduces oscillations that may degrade system efficiency. Additionally, the complexity of designing an appropriate sliding surface and ensuring stability requires extensive mathematical modeling. Compared to SMC, CMC offers smoother control action and easier implementation, albeit with a slightly slower response under extreme load variations.

Predictive Control (Model Predictive Control – MPC) takes a model-based approach, forecasting system behavior and optimizing control inputs in real time. MPC is particularly effective in handling multi-objective control, such as voltage regulation, efficiency optimization, and disturbance rejection. Its major advantages include excellent dynamic performance and precise control, making it suitable for smart grids, electric vehicle (EV) charging systems, and renewable energy applications. However, MPC requires high computational power, as it relies on solving complex equations at each control interval. This makes it less practical for low-cost power converters, where CMC remains a more feasible option due to its lower computational burden and easier implementation.

Fuzzy Logic Control (FLC) is another alternative that relies on linguistic rules and heuristic decision-making rather than mathematical models. FLC is highly adaptable to nonlinear systems and does not require precise modeling, making it beneficial for renewable energy converters where environmental conditions fluctuate unpredictably. However, FLC faces challenges in tuning membership functions and lacks optimality in fast transient response, as it operates more reactively than proactively. Compared to CMC, which provides structured, real-time response control, FLC is better suited for applications where adaptability to unpredictable variations is required rather than stringent performance optimization.

The performance of the proposed converter based on the current mode control scheme is checked by simulating it on MATLAB with the following design parameters:  $V_{in} = 100V$ ,  $V_{out} = 600$ ,  $L_1 = 600\mu H$ ,  $L_2 = 2.4mH$ ,  $R_{1L} = 40\Omega$ ,  $C_1 = 56\mu F$ ,  $f_s = 50kHz$ ,  $D = 0.534$ .

**Table 2.** Component’s selection and relevant values

Parameter	Value	Unit
Inductor $L_1$	600uH	Henry
Inductor $L_2$	2.4mH	Henry
Mutual Inductance	1.14e-3H	Henry
Diode (RHRG75120)	-	-
Mosfet (IRF640N)	-	-

Capacitor	220uF	farad
Input Voltage	100V	volt
Load Resistance	40Ω	ohm
Pulse width (%)	53.4%	-
Operating Frequency	50k	Hz

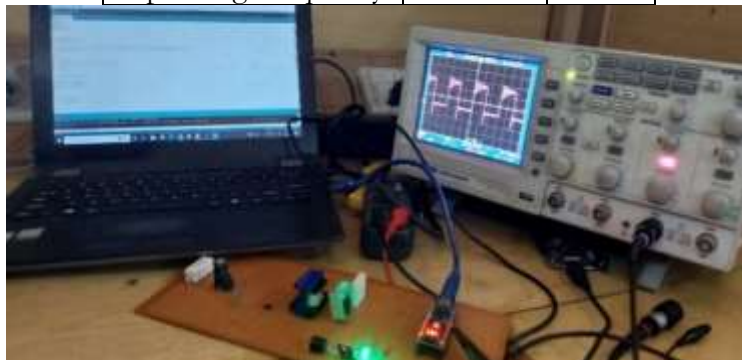


Figure 13. Prototype design implementation for the proposed converter

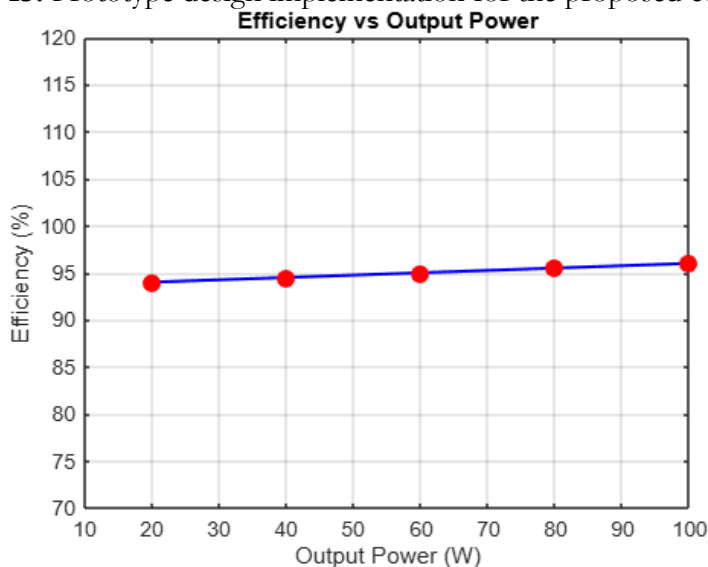


Figure 14. Efficiency vs power at the output (W)

**Conclusion & Future Recommendation:**

Coupled inductors-based boost converters having efficient control are well known to attain regulated voltage at the output. While achieving the goals of high gain and high efficiency. Such step-up high-gain converters can be efficiently integrated with renewable energy resources and electric vehicle applications. Current-injected control (or CMC) is being implemented and presented in this thesis/research work to obtain regulated voltage at the output. A small signal model with average method state space modeling is represented as well. Current-injected mode control (or CMC) is utilized to achieve fast transient response, low THD (total harmonic distortion), input disturbance rejection, and stable DC link. Coupled inductor topology is utilized to obtain high gain by the adjustment of turn’s ratio properly. Renewable resources like solar-based energy generation systems prioritize such converters owing to their variable nature. Such high-gain converters are also helpful in increasing the low voltage obtained from such resources. MPPT (maximum power point tracking) helps to achieve maximum power from the PV panel using perturb and observe technique irrespective of temperature and irradiance. The proposed converter has been implemented on the Matlab Simulink model and it’s also verified via a hardware-based laboratory prototype.

## Recommendations for Future Work:

As a future recommendation the proposed converter can be effectively integrated with EV i.e., electrical vehicle-based applications. With the increase in the rates of fuel and depletion of conventional resources like natural gas, and fossil fuels and likewise, it is mandatory to look for advanced techniques that can help to implement electric cars on a large scale. This step will pay a lot for economic development throughout the world. Another application of the proposed converter involves the penetration of PV (solar arrays) on the source side. There is ongoing research on a wide scale regarding smart grids and microgrids. The variable as well as unreliable nature of PV module system requires such dc-dc converters which can provide voltage regulation. The concept of active building is also under consideration which again emphasizes the requirement of efficient high-gain step-up dc/DC converters.

## References:

- [1] G. Velasco-Quesada, F. Guinjoan-Gispert, R. Piqué-López, M. Román-Lumbreras, and A. Conesa-Roca, "Electrical PV array reconfiguration strategy for energy extraction improvement in grid-connected PV systems," *IEEE Trans. Ind. Electron.*, vol. 56, no. 11, pp. 4319–4331, 2009, doi: 10.1109/TIE.2009.2024664.
- [2] F. Nejabatkhah, S. Danyali, S. H. Hosseini, M. Sabahi, and S. M. Niapour, "Modeling and control of a new three-input dc-dc boost converter for hybrid PV/FC/battery power system," *IEEE Trans. Power Electron.*, vol. 27, no. 5, pp. 2309–2324, 2012, doi: 10.1109/TPEL.2011.2172465.
- [3] M. Forouzesh, Y. Shen, K. Yari, Y. P. Siwakoti, and F. Blaabjerg, "High-Efficiency High Step-Up DC-DC Converter with Dual Coupled Inductors for Grid-Connected Photovoltaic Systems," *IEEE Trans. Power Electron.*, vol. 33, no. 7, pp. 5967–5982, Jul. 2018, doi: 10.1109/TPEL.2017.2746750.
- [4] Y. P. Hsieh, J. F. Chen, T. J. Liang, and L. S. Yang, "A novel high step-up DC-DC converter for a microgrid system," *IEEE Trans. Power Electron.*, vol. 26, no. 4, pp. 1127–1136, 2011, doi: 10.1109/TPEL.2010.2096826.
- [5] R. J. Wai, C. Y. Lin, C. Y. Lin, R. Y. Duan, and Y. R. Chang, "High-efficiency power conversion system for kilowatt-level stand-alone generation unit with low input voltage," *IEEE Trans. Ind. Electron.*, vol. 55, no. 10, pp. 3702–3714, 2008, doi: 10.1109/TIE.2008.921251.
- [6] H. Ardi, A. Ajami, and M. Sabahi, "A novel high step-up DC-DC converter with continuous input current integrating coupled inductor for renewable energy applications," *IEEE Trans. Ind. Electron.*, vol. 65, no. 2, pp. 1306–1315, 2018, doi: 10.1109/TIE.2017.2733476.
- [7] W. Li and X. He, "Review of nonisolated high-step-up DC/DC converters in photovoltaic grid-connected applications," *IEEE Trans. Ind. Electron.*, vol. 58, no. 4, pp. 1239–1250, Apr. 2011, doi: 10.1109/TIE.2010.2049715.
- [8] Q. Zhao and F. C. Lee, "High-efficiency, high step-up dc-dc converters," *IEEE Trans. Power Electron.*, vol. 18, no. 1 I, pp. 65–73, Jan. 2003, doi: 10.1109/TPEL.2002.807188.
- [9] F. Li and H. Liu, "A Cascaded Coupled Inductor-Reverse High Step-Up Converter Integrating Three-Winding Coupled Inductor and Diode-Capacitor Technique," *IEEE Trans. Ind. Informatics*, vol. 13, no. 3, pp. 1121–1130, Jun. 2017, doi: 10.1109/TII.2016.2637371.
- [10] H. M. Hsu and C. T. Chien, "Multiple turn ratios of on-chip transformer with four intertwining coils," *IEEE Trans. Electron Devices*, vol. 61, no. 1, pp. 44–47, 2014, doi: 10.1109/TED.2013.2292855.
- [11] B. Gu, J. Dominic, J. S. Lai, Z. Zhao, and C. Liu, "High boost ratio hybrid transformer DC-DC converter for photovoltaic module applications," *IEEE Trans. Power Electron.*, vol. 28, no. 4, pp. 2048–2058, Apr. 2013, doi: 10.1109/TPEL.2012.2198834.
- [12] T. J. Liang, J. H. Lee, S. M. Chen, J. F. Chen, and L. S. Yang, "Novel isolated high-step-Up DC-DC converter with voltage lift," *IEEE Trans. Ind. Electron.*, vol. 60, no. 4, pp. 1483–1491, 2013, doi: 10.1109/TIE.2011.2177789.
- [13] Y. Tang, D. Fu, T. Wang, and Z. Xu, "Hybrid switched-inductor converters for high step-up conversion," *IEEE Trans. Ind. Electron.*, vol. 62, no. 3, pp. 1480–1490, Mar. 2015, doi: 10.1109/TIE.2014.2364797.
- [14] Y. Tang, T. Wang, and Y. He, "A switched-capacitor-based active-network converter with high

- voltage Gain,” *IEEE Trans. Power Electron.*, vol. 29, no. 6, pp. 2959–2968, Jun. 2014, doi: 10.1109/TPEL.2013.2272639.
- [15] G. Wu, X. Ruan, and Z. Ye, “High Step-Up DC-DC Converter Based on Switched Capacitor and Coupled Inductor,” *IEEE Trans. Ind. Electron.*, vol. 65, no. 7, pp. 5572–5579, Jul. 2018, doi: 10.1109/TIE.2017.2774773.
- [16] H. C. Liu and F. Li, “Novel High Step-Up DC-DC Converter with an Active Coupled-Inductor Network for a Sustainable Energy System,” *IEEE Trans. Power Electron.*, vol. 30, no. 12, pp. 6476–6482, Dec. 2015, doi: 10.1109/TPEL.2015.2429651.
- [17] S. H. C. Taosif Iqbal, Yaqian Wang, Haibin Lu, Xiongwen Zhang, “Small signal modelling and control of high gain coupled inductor boost inverter for solid oxide fuel cell based power generation system,” *Int. J. Hydrogen Energy*, vol. 44, no. 38, pp. 21115–21126, 2019, doi: <https://doi.org/10.1016/j.ijhydene.2019.01.289>.
- [18] A. F. Witulski, “Introduction to Modeling of Transformers and Coupled Inductors,” *IEEE Trans. Power Electron.*, vol. 10, no. 3, pp. 349–357, 1995, doi: 10.1109/63.388001.
- [19] Texas Instruments, “AN-1286 Compensation for the LM3478 Boost Controller,” Application Note. Accessed: Mar. 17, 2025. [Online]. Available: <https://e2e.ti.com/support/power-management-group/power-management/f/power-management-forum/922179/lm3478-an-1286-compensation-for-the-lm3478-boost-controller>
- [20] Texas Instruments, “Demystifying Type II and Type III Compensators Using OpAmp and OTA for DC/DC Converters,” *Appl. Rep.*, 2014, [Online]. Available: <https://www.ti.com/lit/an/slva662/slva662.pdf>
- [21] M. A. Vaghela and M. A. Mulla, “Peak Current Mode Control of Coupled Inductor based High Step-Up Gain Boost Converter,” *India Int. Conf. Power Electron. IICPE*, vol. 2018-December, Jul. 2018, doi: 10.1109/IICPE.2018.8709507.
- [22] Y. P. Hsieh, J. F. Chen, T. J. Liang, and L. S. Yang, “Novel high step-Up DC-DC converter for distributed generation system,” *IEEE Trans. Ind. Electron.*, vol. 60, no. 4, pp. 1473–1482, 2013, doi: 10.1109/TIE.2011.2107721.
- [23] M. B. Meier, D. S. S. Avelino, A. A. Badin, E. F. R. Romaneli, and R. Gules, “Soft-switching high static gain DC-DC converter without auxiliary switches,” *IEEE Trans. Ind. Electron.*, vol. 65, no. 3, pp. 2335–2345, Mar. 2018, doi: 10.1109/TIE.2017.2739684.



Copyright © by authors and 50Sea. This work is licensed under Creative Commons Attribution 4.0 International License.